Available online at www.sciencedirect.com

SCIENCE DIRECT

International Journal of Mechanical Sciences 48 (2006) 907–915

International Journal of MECHANICAL SCIENCES

www.elsevier.com/locate/ijmecsci

In-plane and out-of-plane buckling of arches made of FGM

H. Shafiee[a], M.H. Naei[a], M.R. Eslami[b,*]

[a]Mechanical Engineering Department, Tehran University, Tehran, Iran
[b]Mechanical Engineering Department, Amirkabir University of Technology, Tehran, Iran

Received 22 July 2004; received in revised form 3 January 2006; accepted 28 January 2006
Available online 2 May 2006

Abstract

The mechanical buckling of curved beams made of functionally graded materials is studies in this paper. The equilibrium and stability equations of curved beams under mechanical loads are derived. Using proper approximate functions for the displacement components, the stability equations are employed to obtain the related eigenvalues associated with the buckling load of the curved beam. Closed-form solutions are obtained for mechanical buckling of curved beams with doubly symmetric cross section subjected to uniform distributed radial load and pure bending moment. The results are validated with the known data in the literature for beams with isotropic materials.

Keywords: Curved beam; Arch; Buckling; Functionally graded material

1. Introduction

Research on the buckling of curved beams is a subject of intensive interest. The critical buckling loads of a curved beam, under the uniform bending and uniform compression, are obtained by Timoshenko and Gere [1] using the equilibrium approach. Based on an analogy between the generalized strains for straight and curved members, Vlasov [2] and Yoo [3] started their formulations to obtain the buckling loads of a curved beam from the straight beam theory. By replacing the generalized strains for the straight beam with those of the curved beam, Vlasov [2] worked directly on the equilibrium equations and Yoo [3] proceeded with the potential energy expression followed by a variational procedure. The stability equations and the resulting buckling loads, as achieved by Vlasov and Yoo, are different.

Yang and Kuo [4] applied the principle of virtual displacements to derive the buckling equations of curved beams. Papangelis and Trahair [5] investigated the same problem using the potential energy approach. Rajasekaran and Padmanabhan [6] derived their own equilibrium and stability equations of curved beams based on the principle of virtual work. Kuo and Yang [7] presented a stability theory for symmetric thin-walled curved beams considering the curvature effects. Kang and Yoo [8] derived the analytical solutions for the stability behavior of a simply supported thin-walled curved beam having a doubly symmetric open section. Kim et al. [9] improved the formulation for the spatial stability of curved beams with nonsymmetric cross section based on the displacement field, considering the constant curvature effects and the second-order terms of finite semi-tangential rotations. The in-plane and out-of-plane buckling of steel arches are presented by Refs. [10–12]. The flexural-torsional buckling of steel arches is investigated by Ref. [13].

Functionally graded materials (FGMs) are advanced and heat-resisting materials used in modern technologies as structural elements. FGMs have received considerable attention in many engineering applications since they were first reported in 1984 in Japan. FGMs are heterogeneous materials in which the elastic and thermal properties change from one surface to the other, gradually and continuously. The material is constructed by smoothly changing the volume fraction of the constituent materials. Typically, these materials are made from a mixture of ceramic and metal. With the increased use of these materials in the industry, the behavior of the FGM structures under thermal and mechanical loads are essential.

*Corresponding author. Tel.: +98 21 640 5844; fax: +98 21 641 9736.
E-mail address: eslami@aut.ac.ir (M.R. Eslami).

0020-7403/$ - see front matter
doi:10.1016/j.ijmecsci.2006.01.001

Thermal buckling of rings made of FGMs is presented by Shahsiah and Eslami [14]. Buckling of FGM rectangular plates under axial load, is studied by Briman [15]. Ng et al. [16] derived the stability equations and buckling loads of FGM circular cylindrical shells under axial harmonic loading condition. Thermal and mechanical buckling of FGM plates are studied by Javaheri and Eslami [17–19] and Najafizadeh and Eslami [20–22]. Thermal stability of FGM circular cylindrical shells based on the Donnell stability equations are investigated by Shahsiah and Eslami [25].

In this paper, a curved beam made of FGM is considered. The Reddy's model for the variation of the modules of elasticity is considered for the material distribution across the thickness of the curved beam. The equilibrium and stability equations of curved beams under mechanical loads are derived using the variational principle. The closed-form solutions for buckling load related to the uniform compression and pure bending moment are obtained. The results are reduced to the mechanical buckling loads of curved beams made of isotropic materials.

2. Linearized Helinger–Reissner principle

The Helinger–Reissner principle for a general continuum subjected to surface forces is expressed as

$$\delta\left\{\int_V {}^t\tau_{ij}\,{}^t\varepsilon_{ij}\,\mathrm{d}V - \int_S {}^tT_i\,{}^tu_i\,\mathrm{d}S\right\} = 0, \tag{1}$$

where ${}^t\tau_{ij}$ is the second Piola–Kirchhoff stress tensor, ${}^t\varepsilon_{ij}$ is the Green–Lagrange strain tensor, ${}^tT_i$ and ${}^tu_i$ are the surface force and displacement vector, respectively. The sign δ refers to the first variation and the superscript t indicates the total variables. Total variables are decomposed into the initial and incremental variables as

$${}^tu_i = u_i + u_i^*, \quad {}^t\varepsilon_{ij} = \varepsilon_{ij} = e_{ij} + \eta_{ij} + e_{ij}^*, \tag{2}$$

$${}^t\tau_{ij} = {}^0\tau_{ij} + \tau_{ij}, \quad {}^tT_i = {}^0T_i + T_i, \tag{3}$$

where the superscript 0 represents the value the terms satisfying the equilibrium equations. The terms with no superscript represent the incremental variables. Here, u_i and u_i^* denote the first-order and second-order terms of the displacement components, respectively. Also, e_{ij}, η_{ij}, and e_{ij}^* are the conventional linear, the nonlinear, and the linear strain increment due to the first- and second-order terms of the displacement components, respectively. The Green–Lagrange strains, including the second-order displacement terms, are expressed as

$$\begin{aligned}\varepsilon_{ij} = \tfrac{1}{2}\{&(u_i + u_i^*)_{,j} + (u_j + u_j^*)_{,i} \\ &+ (u_k + u_k^*)_{,i} + (u_k + u_k^*)_{,j}\}\end{aligned} \tag{4}$$

in which

$$e_{ij} = \tfrac{1}{2}(u_{i,j} + u_{j,i}), \quad \eta_{ij} = \tfrac{1}{2}u_{k,i}.u_{k,j}, \tag{5}$$

$$e_{ij}^* = \tfrac{1}{2}(u_{i,j}^* + u_{j,i}^*). \tag{6}$$

The constraint equation of the self-equilibrating initial stress and surface forces is [23]

$$\int_V^0 \tau_{ij}e_{ij}\,\mathrm{d}V = \int_S^0 T_i\delta u_i\,\mathrm{d}s. \tag{7}$$

Substituting Eqs. (2), (3), and (7) into (1) and neglecting terms of order three and higher, the linearized Helinger–-Reissner principle for the general continuum subjected to initial stresses is express

$$\begin{aligned}\delta\Bigg\{&\int_V [\tau_{ij}e_{ij} + {}^0\tau_{ij}(\eta_{ij} + e_{ij}^*)]\,\mathrm{d}V \\ &- \int_S^0 T_iu_i^*\,\mathrm{d}s - \int_S T_iu_i\,\mathrm{d}s\Bigg\} = 0.\end{aligned} \tag{8}$$

2.1. Displacement field of cross section

Displacement parameters for a thin-walled cross section arch with right-handed coordinate system are shown in Fig. 1. The x_1-axis coincides with the centroid of the cross section, x_2, and x_3 are the principle inertia axes, u_x, u_y, u_z are the rigid body translations of the cross section along the x_1-, x_2-, x_3-direction at the centroid and w_1, w_2, w_3 are the rigid body rotations about the centroid x_2- and x_3-direction, respectively.

Since the shear deformation is assumed to be negligible, the expressions for the rigid body rotations w_2, w_3 and the warping parameter f may be derived from the Frent's formula [6] as

$$w_2 = -u_z' + \frac{u_x}{R}, \quad w_3 = u_y', \tag{9}$$

$$f = -\theta' - \frac{u_y'}{R}. \tag{10}$$

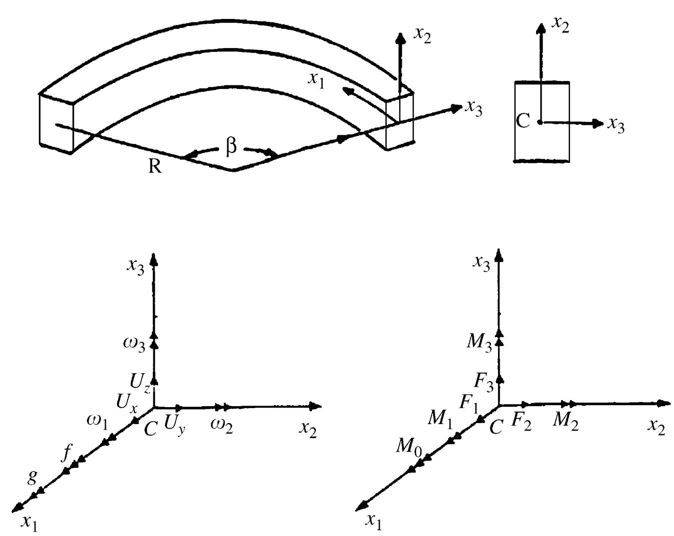

Fig. 1. Coordinate system, notation of displacement parameters, and stress results.

In addition, we define the functions g and ψ as

$$g = u'_x + \frac{u_z}{R}, \quad \psi = u''_y - \frac{\theta}{R}, \tag{11}$$

where the superscript prime indicates the derivative with respect to x_1, $\theta = w_1$, and R is the centroid radius of the arch. The derivation procedure for the displacement field including the second-order terms of finite rotations are given in the previous studies by Kim et al. [9]. The total displacement field according to Kim et al. is expressed as

$$u_1 = u_x - x_2 u'_y - x_3\left(u'_z - \frac{u_x}{R}\right) - \left(\theta' + \frac{u'_y}{R}\right)\varphi(x_2, x_3), \tag{12}$$

$$u_2 = u_y - x_3\theta, \quad u_3 = u_z + x_2\theta, \tag{13}$$

$$u_1^* = \frac{1}{2}\left[-\theta\left(u'_z - \frac{u_x}{R}\right)x_2 + \theta u'_y x_3\right], \tag{14}$$

$$u_2^* = \frac{1}{2}\left[-(\theta^2 + u'^2_y)x_2 - \left(u'_z - \frac{u_x}{R}\right)u'_y x_3\right], \tag{15}$$

$$u_3^* = \frac{1}{2}\left[-\left(u'_z - \frac{u_x}{R}\right)u'_y x_2 - \left\{\theta^2 + \left(u'_z - \frac{u_x}{R}\right)^2\right\}x_3\right], \tag{16}$$

where $\varphi(x_2, x_3)$ is the warping function defined at the centroid.

The section properties of the curved beam may be defined as

$$\begin{aligned}
&I_2 = \int_A x_3^2\,\mathrm{d}A, \quad I_3 = \int_A x_2^2\,\mathrm{d}A, \quad I_{23} = \int_A x_2 x_3\,\mathrm{d}A,\\
&I_\varphi = \int_A \varphi^2\,\mathrm{d}A, \quad I_{\varphi 2} = \int_A \varphi x_3\,\mathrm{d}A, \quad I_{\varphi 3} = \int_A \varphi x_2\,\mathrm{d}A,\\
&I_{222} = \int_A x_3^3\,\mathrm{d}A, \quad I_{223} = \int_A x_2 x_3^2\,\mathrm{d}A, \quad I_{233} = \int_A x_3 x_2^2\,\mathrm{d}A,\\
&I_{333} = \int_A x_2^3\,\mathrm{d}A, \quad I_{\varphi 22} = \int_A \varphi x_3^2\,\mathrm{d}A, \quad I_{\varphi 33} = \int_A \varphi x_2^2\,\mathrm{d}A,\\
&I_{\varphi 23} = \int_A \varphi x_2 x_3\,\mathrm{d}A, \quad I_{\varphi\varphi 2} = \int_A \varphi^2 x_3\,\mathrm{d}A,\\
&I_{\varphi\varphi 3} = \int_A \varphi^2 x_2\,\mathrm{d}A, \quad \hat{I}_2 = I_2 - \frac{I_{222}}{R},\\
&\hat{I}_3 = I_3 - \frac{I_{233}}{R}, \quad \hat{I}_\varphi = I_\varphi - \frac{I_{\varphi\varphi 2}}{R},\\
&\hat{I}_{\varphi 2} = I_{\varphi 2} - \frac{I_{\varphi 22}}{R}, \quad \hat{I}_{\varphi 3} = I_{\varphi 3} - \frac{I_{\varphi 23}}{R},\\
&\hat{I}_{23} = I_{23} - \frac{I_{223}}{R}.
\end{aligned} \tag{17}$$

For an arch with doubly symmetric cross section, the section properties I_{23}, $I_{\phi 2}$, $I_{\phi 3}$, I_{222}, I_{223}, I_{233}, I_{333}, $I_{\phi 22}$, $I_{\phi 33}$, $I_{\phi 23}$, $I_{\phi\phi 2}$, $I_{\phi\phi 3}$ become zero.

2.2. Strain–displacement relations and stress results

Complete linear strain–displacement relations due to the first-order displacement parameters based on Eq. (5), using Eqs. (12) and (13), are

$$\begin{aligned}
e_{11} = \Bigg[&u'_x + \frac{u_z}{R} - x_2\left(u''_y - \frac{\theta}{R}\right)\\
&- x_3\left(u''_z - \frac{u'_x}{R}\right) - \varphi\left(\theta'' + \frac{u''_y}{R}\right)\Bigg]\frac{R}{R + x_3},
\end{aligned} \tag{18}$$

$$2e_{12} = -x_3\left(\theta' + \frac{u'_y}{R}\right)\frac{R}{R + x_3} - \left(\theta' + \frac{u'_y}{R}\right)\varphi_{,2}, \tag{19}$$

$$2e_{13} = \left(x_2 + \frac{\varphi}{R}\right)\left(\theta' + \frac{u'_y}{R}\right)\frac{R}{R + x_3} - \left(\theta' + \frac{u'_y}{R}\right)\varphi_{,3}, \tag{20}$$

where ϕ_2 and ϕ_3 are the derivatives of ϕ with respect to x_2 and x_3, respectively, and the nonlinear strain–displacement relations due to the first-order displacement parameters based on Eqs. (5) and (6), using Eqs. (12)–(16), are

$$\begin{aligned}
\eta_{11} = \frac{1}{2}\Bigg[&\Bigg\{u'_x + \frac{u_z}{R} - x_2\left(u''_y - \frac{\theta}{R}\right)\\
&- x_3\left(u''_z - \frac{u'_x}{R}\right) - \varphi\left(\theta'' + \frac{u''_y}{R}\right)\Bigg\}^2\\
&+ \{u'_y - x_3\theta'\}^2 + \Bigg\{u'_z + x_2\theta' - \frac{1}{R}u_x\\
&+ \frac{1}{R}x_2 u'_y + \frac{1}{R}x_3\left(u'_z - \frac{u_x}{R}\right)\\
&+ \frac{1}{R}\varphi\left(\theta' + \frac{u'_y}{R}\right)\Bigg\}^2\Bigg]\left(\frac{R}{R + x_3}\right)^2,
\end{aligned} \tag{21}$$

$$\begin{aligned}
\eta_{12} = \frac{1}{2}\Bigg[&-u'_y\Bigg\{u'_x + \frac{u_z}{R} - x_2\left(u''_y - \frac{\theta}{R}\right)\\
&- x_3\left(u''_z - \frac{u'_x}{R}\right) - \varphi\left(\theta'' + \frac{u''_y}{R}\right)\Bigg\}\\
&+ \theta\Bigg\{u'_z + x_2\theta' - \frac{1}{R}u_x + \frac{1}{R}x_2 u'_y\\
&+ \frac{1}{R}x_3\left(u'_z - \frac{u_x}{R}\right) + \frac{1}{R}\varphi\left(\theta' + \frac{u'_y}{R}\right)\Bigg\}\Bigg]\left(\frac{R}{R + x_3}\right),
\end{aligned} \tag{22}$$

$$\begin{aligned}
\eta_{13} = \frac{1}{2}\Bigg[&-\left(u'_z - \frac{u_x}{R}\right)\Bigg\{u'_x + \frac{u_z}{R} - x_2\left(u''_y - \frac{\theta}{R}\right)\\
&- x_3\left(u''_z - \frac{u'_x}{R}\right) - \varphi\left(\theta'' + \frac{u''_y}{R}\right)\Bigg\}\\
&- \theta(u''_y - x_3\theta')\Bigg]\frac{R}{R + x_3},
\end{aligned} \tag{23}$$

$$\begin{aligned}
e^*_{11} = \frac{1}{2}\Bigg[&x_2\left\{\theta\left(u'_z - \frac{u_x}{R}\right)\right\}'\\
&+ \frac{1}{2R}x_2 u'_y\left(u'_z - \frac{u_x}{R}\right) + x_3(\theta u'_y)'\\
&- \frac{1}{2R}x_3\theta^2 - \frac{1}{2R}x_3\left(u'_z - \frac{u_x}{R}\right)^2\Bigg]\frac{R}{R + x_3},
\end{aligned} \tag{24}$$

$$2e_{12}^{*}=\frac{1}{2}\left[-(\theta^{2}+u_{y}'^{2})'x_{2}-\left(u_{z}''-\frac{u_{x}'}{R}\right)u_{y}'x_{3}-\left(u_{z}'-\frac{u_{x}}{R}\right)u_{y}''x_{3}\right]\frac{R}{R+x_{3}}-\frac{1}{2}\theta\left(u_{z}'-\frac{u_{x}}{R}\right),\qquad(25)$$

$$2e_{13}^{*}=\frac{1}{2}\left[\left\{-\left(u_{y}'\left(u_{z}'-\frac{u_{x}}{R}\right)\right)'x_{2}-\left\{\theta^{2}+\left(u_{z}'-\frac{u_{x}}{R}\right)^{2}\right\}'x_{3}\right\}-\frac{1}{2R}\left\{\theta x_{2}\left(u_{z}'-\frac{u_{x}}{R}\right)+\theta u_{y}'x_{3}\right\}\right]\frac{R}{R+x_{3}}+\frac{1}{2}\theta u_{y}'.\qquad(26)$$

Assuming the rigid in-plane deformation state, the incremental stress resultants may be defined as

$$F_{1}=\int_{A}\tau_{11}\,\mathrm{d}A,\quad F_{2}=\int_{A}\tau_{12}\,\mathrm{d}A,\quad F_{3}=\int_{A}\tau_{13}\,\mathrm{d}A,\qquad(27)$$

$$M_{2}=\int_{A}\tau_{11}x_{3}\,\mathrm{d}A,\quad M_{3}=-\int_{A}\tau_{11}x_{2}\,\mathrm{d}A,\quad M_{\varphi}=\int_{A}\tau_{11}\varphi\,\mathrm{d}A,\quad M_{1}=\int_{A}(\tau_{13}x_{2}-\tau_{12}x_{3})\,\mathrm{d}A.\qquad(28)$$

Now, a functionally graded beam made of ceramic and metal is considered. In Eqs. (27) and (28), the material properties of the FGM beam must be considered. The beam is assumed to be graded across the thickness, along the x_3-direction. The linearized form of the material properties proposed by Praveen and Reddy [24] are assumed as

$$E(x_{3})=E_{m}+E_{cm}\left(\frac{2x_{3}+h}{2h}\right)=\bar{E}+\frac{E_{cm}}{h}x_{3},\qquad(29)$$

$$v(x_{3})=v_{0},\qquad(30)$$

where E_m and E_c are the modulus of elasticity of the metal and ceramic constituent materials of the beam, respectively. The Poisson's ratio v of metal and ceramic are assumed to be identical. Term E_{cm} is

$$E_{cm}=E_{c}-E_{m},\quad \bar{E}=\tfrac{1}{2}(E_{c}+E_{m}),\quad \alpha_{cm}=\alpha_{c}-\alpha_{m}.\qquad(31)$$

Here, substituting Eqs. (28) and (31) in Eqs. (26) and (27) and simplifying the results, give the final expression for stress results as

$$F_{1}=\left[\bar{E}\left(A+\frac{1}{R^{2}}\hat{I}_{2}\right)+E_{cm}\left(-\frac{1}{Rh}\hat{I}_{2}\right)\right]\mathrm{g}+\left[\bar{E}\left(\frac{1}{R}\hat{I}_{23}\right)+E_{cm}\left(-\frac{1}{h}\hat{I}_{23}\right)\right]\psi+\left[\bar{E}\left(-\frac{1}{R}\hat{I}_{2}\right)+E_{cm}\left(\frac{1}{h}\hat{I}_{2}\right)\right]w_{2}'+\left[\bar{E}\left(-\frac{1}{R}\hat{I}_{\varphi 2}\right)+E_{cm}\left(\frac{1}{h}\hat{I}_{\varphi 2}\right)\right]f',\qquad(32)$$

$$M_{2}=\left[\bar{E}\left(-\frac{1}{R}\hat{I}_{2}\right)+E_{cm}\left(\frac{1}{h}\hat{I}_{2}\right)\right]\mathrm{g}+\left[\bar{E}(-\hat{I}_{23})+E_{cm}\left(-\frac{1}{h}I_{223}\right)\right]\psi+\left[\bar{E}(\hat{I}_{2})+E_{cm}\left(\frac{1}{2}I_{222}\right)\right]w_{2}'+\left[\bar{E}(\hat{I}_{\varphi 2})+E_{cm}\left(\frac{1}{h}\hat{I}_{\varphi 22}\right)\right]f',\qquad(33)$$

$$M_{3}=\left[\bar{E}\left(\frac{1}{R}\hat{I}_{23}\right)+E_{cm}\left(-\frac{1}{h}\hat{I}_{23}\right)\right]\mathrm{g}+\left[\bar{E}(\hat{I}_{3})+E_{cm}\left(\frac{1}{h}\hat{I}_{233}\right)\right]\psi+\left[\bar{E}(-\hat{I}_{23})+E_{cm}\left(-\frac{1}{h}I_{223}\right)\right]w_{2}'+\left[\bar{E}(-\hat{I}_{3\varphi})+E_{cm}\left(\frac{1}{h}\hat{I}_{23\varphi}\right)\right]f',\qquad(34)$$

$$M_{\varphi}=\left[\bar{E}\left(-\frac{1}{R}\hat{I}_{\varphi 2}\right)+E_{cm}\left(\frac{1}{h}\hat{I}_{\varphi 2}\right)\right]\mathrm{g}+\left[\bar{E}(-\hat{I}_{\varphi 3})+E_{cm}\left(-\frac{1}{h}\hat{I}_{23\varphi}\right)\right]\psi+\left[\bar{E}(\hat{I}_{\varphi 2})+E_{cm}\left(\frac{1}{h}I_{\varphi 22}\right)\right]w_{2}'+\left[\bar{E}(\hat{I}_{\varphi})+E_{cm}\left(\frac{1}{h}I_{\varphi\varphi 2}\right)\right]f'.\qquad(35)$$

3. Total potential energy of curved beams

The total potential energy of a curved beam subjected to mechanical forces and moments, consisting of elastic strain energy Π_E and the potential energy of external forces Π_{G_1} and Π_{G_2} may be written as

$$\Pi_{E}=\frac{1}{2}\int_{0}^{L}\int_{A}[s_{11}e_{11}+2s_{12}e_{12}+2s_{13}e_{13}]\frac{R+x_{3}}{R}\,\mathrm{d}A\,\mathrm{d}x_{1},\qquad(36)$$

$$\Pi_{G_1}=\frac{1}{2}\int_{0}^{L}\int_{A}[{}^{0}\tau_{11}\eta_{11}+2\,{}^{0}\tau_{12}\eta_{12}+2\,{}^{0}\tau_{13}\eta_{13}]\frac{R+x_{3}}{R}\,\mathrm{d}A\,\mathrm{d}x_{1},\qquad(37)$$

$$\Pi_{G_2}=\frac{1}{2}\int_{0}^{L}\int_{A}[{}^{0}\tau_{11}e_{11}^{*}+2\,{}^{0}\tau_{12}e_{12}^{*}+2\,{}^{0}\tau_{13}e_{13}^{*}]\frac{R+x_{3}}{R}\,\mathrm{d}A\,\mathrm{d}x_{1}.\qquad(38)$$

Substituting the linear strain–displacement relations (17)–(19) into Eq. (36), considering the Hooke's law modified for the FGM beam, and integrating over the cross section of the beam, the elastic strain energy Π_E is derived as

$$\Pi_E = \frac{1}{2}\int_0^L \Bigg[\bar{E}A\left(u'_x + \frac{u_z}{R}\right)^2 + \bar{E}\hat{I}_3\left(u''_z - \frac{u'_x}{R}\right)\left(u''_y - \frac{\theta}{R}\right)$$
$$+ 2\bar{E}\hat{I}_{3\varphi}\left(\theta'' + \frac{u''_y}{R}\right)\left(u''_y - \frac{\theta}{R}\right) + \bar{E}\hat{I}_2\left(u''_z - \frac{u'_x}{R}\right)^2$$
$$+ 2\bar{E}\hat{I}_{\varphi 2}\left(\theta'' + \frac{u''_y}{R}\right)\left(u''_z - \frac{u'_x}{R}\right) + \bar{E}\hat{I}_\varphi\left(\theta'' + \frac{u''_y}{R}\right)^2$$
$$- \frac{E_{cm}}{h}\hat{I}_{23}\left(u''_y - \frac{\theta}{R}\right)\left(u'_x + \frac{u_z}{R}\right)$$
$$+ \frac{E_{cm}}{h}\hat{I}_2\left(-u''_z + \frac{u'_x}{R}\right)\left(u''_y + \frac{u_z}{R}\right)$$
$$+ \frac{E_{cm}}{h}\hat{I}_{\varphi 2}\left(-\theta'' - \frac{u''_y}{R}\right)\left(u'_x + \frac{u_z}{R}\right)$$
$$- \frac{E_{cm}}{h}\hat{I}_{23}\left(u'_x + \frac{u_z}{R}\right)\left(u''_y + \frac{\theta}{R}\right) + \frac{E_{cm}}{h}\hat{I}_{233}\left(u''_y - \frac{\theta}{R}\right)^2$$
$$+ \frac{E_{cm}}{h}\hat{I}_{223}\left(u''_z - \frac{u'_x}{R}\right)\left(u''_y - \frac{\theta}{R}\right)$$
$$- \frac{E_{cm}}{h}\hat{I}_{23\varphi}\left(\theta'' + \frac{u''_y}{R}\right)\left(u''_y - \frac{\theta}{R}\right) + \frac{E_{cm}}{h}\hat{I}_{222}\left(u''_z - \frac{u'_x}{R}\right)^2$$
$$+ \frac{E_{cm}}{h}\hat{I}_{\varphi 22}\left(\theta'' + \frac{u''_y}{R}\right)\left(u''_z - \frac{u'_x}{R}\right)$$
$$- \frac{E_{cm}}{h}\hat{I}_{\varphi 2}\left(u'_x + \frac{u_z}{R}\right)\left(\theta'' + \frac{u''_y}{R}\right)$$
$$+ \frac{E_{cm}}{h}\hat{I}_{23\varphi}\left(u''_y - \frac{\theta}{R}\right)\left(\theta'' + \frac{u''_y}{R}\right)$$
$$- \frac{E_{cm}}{h}\hat{I}_{\varphi 22}\left(-u''_z + \frac{u'_x}{R}\right)\left(\theta'' + \frac{u''_y}{R}\right)$$
$$+ \frac{E_{cm}}{h}\hat{I}_{\varphi\varphi 2}\left(\theta'' + \frac{u''_y}{R}\right) + GJ\left(\theta' + \frac{u'_y}{R}\right)\Bigg]\,\mathrm{d}x_1. \tag{39}$$

To derive the expression for Π_{G_1} and Π_{G_2}, the inextensibility condition and the thickness-curvature effects are considered as

$$u'_x + \frac{u_z}{R} \cong 0, \tag{40}$$

$$\frac{R}{R + x_3} = 1 - \frac{x_3}{R} + \frac{x_3^2}{R^2}. \tag{41}$$

Substituting the strain–displacement relations from Eqs. (20)–(25) into Eqs. (37) and (38) considering the inextensibility condition (40) and the thickness-curvature effect (41), the expression for Π_{G_1} and Π_{G_2} are derived. The final expression for the potential energy functional Π_G is represented as

$$\Pi_G = \frac{1}{2}\int_0^L \Bigg[{}^0F_1\left\{u'^2_y + \left(u'_z - \frac{u_x}{R}\right)^2\right\}$$
$$+ {}^0M_P\left(\theta' + \frac{u'_y}{R}\right)^2 - {}^0F_3(u'_y\theta)$$
$$+ {}^0M_2\left\{\left(u''_y - \frac{\theta}{R}\right)\theta - u'_y\left(\theta' + \frac{u'_y}{R}\right)\right\}$$
$$+ \frac{2\,{}^0M_\varphi}{R}\left(u'_z - \frac{u_x}{R}\right)\left(\theta' + \frac{u'_y}{R}\right)$$
$$+ {}^0M_3\left\{\left(u''_z - \frac{u'_x}{R}\right)\theta - \left(u'_z - \frac{u_x}{R}\right)\left(\theta' + \frac{u'_y}{R}\right)\right\}$$
$$+ {}^0F_2\theta\left(u'_z - \frac{u_x}{R}\right) + {}^0M_1\left\{\left(u'_z - \frac{u_x}{R}\right)\left(u''_y - \frac{\theta}{R}\right)\right.$$
$$\left.\left. - u'_y\left(u''_z - \frac{u'_x}{R}\right)\right\}\right]\mathrm{d}x_1, \tag{42}$$

where G is defined as

$$G = \frac{E(x_3)}{2(1+\upsilon)} = \frac{\bar{E} + (E_{cm}/h)x_3}{2(1+\upsilon)}. \tag{43}$$

4. In-plane buckling

The in-plane buckling problem of circular curved arches subjected to uniformly distributed radial loads q is investigated. Only the terms relevant to the in-plane displacement component from Eqs. (39) and (42) are considered in the expression of total potential energy functional given by

$$\Pi_{in} = \frac{1}{2}\int_0^L \left[\bar{E}I_2\left(Ru''_z + \frac{u_z}{R^2}\right)^2 + {}^0F_1\left(u'_z - \frac{u_x}{R}\right)^2\right]\mathrm{d}x_1. \tag{44}$$

Considering the inextensibility condition (40), total potential energy may be rewritten as

$$\Pi_{in} = \frac{1}{2}\int_0^L \Bigg[\bar{E}I_2\left(Ru'''_x + \frac{u'_x}{R}\right)^2$$
$$+ {}^0F_1R^2\left(u''_x - \frac{u_x}{R^2}\right)^2\Bigg]\mathrm{d}x_1. \tag{45}$$

To derive the second variation of the potential energy function, a perturbation for u_x is considered as

$$u_x = u_{x_0} + u_{x_1} = u_{x_0} + \varepsilon\xi_{(x)}, \tag{46}$$

where ε is a constant value and $\xi_{(x)}$ is a function that satisfies the given boundary conditions and the continuity conditions. The derivatives of the perturbed terms are

$$u'_x = u'_{x_0} + \varepsilon\xi'_{(x)},$$
$$u''_x = u''_{x_0} + \varepsilon\xi''_{(x)},$$
$$u'''_x = u'''_{x_0} + \varepsilon\xi'''_{(x)}. \tag{47}$$

These terms are substituted in Eq. (45) and ignoring the terms with higher order than second-order powers, the second variation of the potential energy is obtained and is

$$\frac{1}{2}\delta^2\Pi = \frac{1}{2}\varepsilon^2\int_0^L \Bigg[\bar{E}I_2\left(R^2\xi'''^2_{(x)} + \frac{1}{R^2}\xi'^2_{(x)} + 2\xi'''_{(x)}\xi'_{(x)}\right)$$
$$+ {}^0F_1R^2\left(\xi''^2_{(x)} + \frac{1}{R^4}\xi^2_{(x)} - \frac{2}{R^2}\xi''_{(x)}\xi_{(x)}\right)\Bigg]\mathrm{d}x_1 \tag{48}$$

$$= \frac{1}{2}\int_0^L \left[\bar{E}I_2\left(R^2 u_{x_1}'''^{\,2} + \frac{1}{R^2}u_{x_1}'^{\,2} + 2u_{x_1}''' u_{x_1}'\right) + {}^0F_1 R^2\left(u_{x_1}''^{\,2} + \frac{1}{R^4}u_{x_1}^2 - \frac{2}{R^2}u_{x_1}'' u_{x_1}\right)\right] \mathrm{d}x_1. \quad (49)$$

The stability equation is obtained from the second variation of the potential energy function as

$$\delta(\delta^2 \Pi) = 0. \quad (50)$$

Using the Euler equation and applying to the functional of the second variation of the potential energy function results into the expression for the stability equation given by

$$(R^4 u_{x_1}^{(vi)} + 2R^2 u_{x_1}^{(iv)} + u_{x_1}'') + K^2\left(R^2 u_{x_1}^{(iv)} + 2u_{x_1}'' + \frac{u_{x_1}}{R^2}\right) = 0, \quad (51)$$

where

$${}^0F_1 = qR, \quad K^2 = \frac{qR^3}{\bar{E}I_2}. \quad (52)$$

The general solution of the above equation is obtained as

$$u_{x_1} = A\cos\frac{x_1}{R} + B\sin\frac{x_1}{R} + Cx_1\cos\frac{x_1}{R} + Dx_1\sin\frac{x_1}{R} + E\cos\frac{Kx_1}{R} + F\sin\frac{Kx_1}{R}, \quad -\frac{L}{2} \leqslant x_1 \leqslant \frac{L}{2}. \quad (53)$$

Since the assumed geometric and loading conditions of the curved beam are symmetric with respect to the x_1-axis, the solution given by expression (53) may be rewritten as

$$u_{x_1} = A\cos\frac{x_1}{R} + Dx_1\sin\frac{x_1}{R} + E\cos\frac{Kx_1}{R}, \quad -\frac{L}{2} \leqslant x_1 \leqslant \frac{L}{2}. \quad (54)$$

For the simply supported ends, the boundary conditions are expressed by

$$u_{x_1}|_{x_1=\pm L/2} = 0, \quad u_{x_1}'|_{x_1=\pm L/2} = 0, \quad u_{x_1}'''|_{x_1=\pm L/2} = 0. \quad (55)$$

Using the above conditions on u_{x_1}, a system of three homogeneous equations are obtained to give

$$\begin{bmatrix} \cos\alpha & \frac{L}{2}\sin\alpha & \cos K\alpha \\ -\frac{1}{R}\sin\alpha & \sin\alpha + \frac{L}{2R}\cos\alpha & -\frac{K}{R}\sin K\alpha \\ \frac{1}{R^3}\sin\alpha & -\frac{3}{R^2}\sin\alpha - \frac{L}{2R^3}\cos\alpha & \frac{K^3}{R^3}\sin K\alpha \end{bmatrix}\begin{bmatrix} A \\ B \\ C \end{bmatrix} = \begin{bmatrix} 0 \\ 0 \\ 0 \end{bmatrix}, \quad (56)$$

where $\alpha = L/2R$. Setting the determinant of Eqs. (56) equal to zero, the following equation is obtained

$$K^3\sin\alpha\cos\alpha\sin K\alpha + K^3\alpha\sin K\alpha - 3K\sin\alpha\cos\alpha\sin K\alpha - K\alpha\sin K\alpha + 2\sin^2\alpha\cos K\alpha = 0. \quad (57)$$

The radial in-plane buckling load is obtained by solving Eq. (57) for the value of K, where the buckling load is included in the expression for K form Eq. (52).

5. Out-of-plane buckling

By retaining only terms that are relevant to the lateral displacement u_y and the torsional rotation θ in Eqs. (39) and (42), the total potential energy function corresponding to the out-of-plane buckling is obtained as

$$\Pi_{out} = \frac{1}{2}\int_0^L \left[\bar{E}I_3\left(u_y'' - \frac{\theta}{R}\right)^2 + \bar{E}I_\varphi\left(\theta'' + \frac{u_y''}{R}\right)^2 + \frac{\bar{E}}{2(1+\upsilon)}J\left(\theta' + \frac{u_y'}{R}\right)^2 + {}^0M_P\left(\theta' + \frac{u_y'}{R}\right)^2 + {}^0M_P\left\{\left(u_y'' - \frac{\theta}{R}\right)\theta - u_y'\left(\theta' + \frac{u_y'}{R}\right)\right\}\right]. \quad (58)$$

Referring to the studies of Kim et al. [9], ${}^0M_P$ may be written as

$${}^0M_P = \beta_1 F_1 + \beta_2 M_2 + \beta_3 M_3 + \beta_\varphi M_\varphi, \quad (59)$$

where the coefficients are given by

$$\beta_1 = \frac{I_2 + I_3}{A}, \quad \beta_2 = \frac{\beta_1}{R} + \frac{I_{222} + I_{233}}{RI_2}, \quad \beta_3 = \frac{I_{\varphi 33} I_{\varphi 3}}{I_3 I_\varphi - I_{\varphi 3}^2}, \quad \beta_\varphi = \frac{I_{\varphi 33} I_3}{I_3 I_\varphi - I_{\varphi 3}^2}. \quad (60)$$

For the stability analysis of doubly symmetric cross section curved beams subjected to in-plane forces, M_P in Eq. (60) is reduced to

$$M_P = \beta_2 M_2 = \frac{\beta_1}{R}M_2 = \frac{I_2 + I_3}{AR}M_2. \quad (61)$$

The lateral displacement and torsional rotation for lateral buckling of simply supported circular arches may be assumed as

$$u_y = B\sin\lambda x_1, \quad \theta = D\sin\lambda x_1, \quad (62)$$

where $\lambda = n\pi/L$. Substituting the displacement function into Eq. (59), the following characteristics equations is obtained by invoking the stationary of Π with respect to the unknown coefficients

$$\begin{bmatrix} A_{11} & A_{12} \\ A_{21} & A_{22} \end{bmatrix}\begin{bmatrix} B \\ D \end{bmatrix} = \begin{bmatrix} 0 \\ 0 \end{bmatrix}, \quad (63)$$

where

$$A_{11} = \bar{E}I_3\lambda^4 + \frac{\bar{E}}{2(1+\upsilon)}J\frac{\lambda^2}{R^2} + \bar{E}I_\varphi\frac{\lambda^4}{R^2} + {}^0M_2\lambda^2\left(\frac{\beta_2}{R^2} - \frac{1}{R}\right), \quad (64)$$

$$A_{12} = \bar{E}I_3\frac{\lambda^2}{R} + \frac{\bar{E}}{2(1+\upsilon)}J\frac{\lambda^2}{R} + \bar{E}I_\varphi\frac{\lambda^4}{R} + {}^0M_2\lambda^2\left(\frac{\beta_2}{R} - 1\right), \quad (65)$$

$$A_{12} = A_{21}, \quad (66)$$

$$A_{22} = \bar{E}I_3\frac{1}{R^2} + \frac{\bar{E}}{2(1+\upsilon)}J\lambda^2 + \bar{E}I_\varphi\lambda^4 + {}^0M_2\left(\beta_2\lambda^2 - \frac{1}{R}\right). \quad (67)$$

To obtain the nontrivial solution of Eq. (63), the determinant of the coefficients is set equal to zero. This leads to a quadratic equation in terms of ${}^0M_2$ given by

$$A_1^0M_{cr}^2 + A_2^0M_{cr}^2 + A_3 = 0, \quad (68)$$

where ${}^0F_1$ was set equal to zero, and

$$A_1 = \left(1 - \frac{\beta_2}{R}\right), \quad (69)$$

$$A_2 = \bar{E}I_3\left(\beta_2\gamma + \frac{1}{R}\right) + \frac{\bar{E}}{2(1+\upsilon)R}J + \bar{E}I_\varphi\frac{\lambda^2}{R}, \quad (70)$$

$$A_3 = \gamma\left[\bar{E}I_3\frac{\bar{E}}{2(1+\upsilon)}J + \bar{E}I_\varphi\lambda^2\right], \quad (71)$$

$$\gamma = \lambda^2 - \frac{1}{R^2}. \quad (72)$$

The out-of-plane buckling moment of the FGM curved beam is obtained from the solution of Eq. (68) for M_{cr}.

6. Results

A ceramic-metal functionally graded curved beam is considered. The material and geometric properties are given as

$$L = 45\,000\,\text{mm}, \quad A = 1440\,\text{mm}^2,$$
$$J = 14\,140\,\text{mm}^4, \quad I_2 = 930\,000\,\text{mm}^4,$$
$$I_3 = 2\,730\,000\,\text{mm}^4, \quad I_\varphi = 2070 \times 10^6\,\text{mm}^6,$$
$$E_m = 27\,880\,\text{N/mm}^2, \quad E_c = 380\,000\,\text{N/mm}^2, \quad \upsilon = 0.3.$$

Using the data given above, a functionally graded curved beam is considered and the related mechanical buckling loads are obtained, using Eq. (57). To validate the results, the analytical solution presented in this study is reduced for the isotropic material (metal) and the resulting expression

Table 1
Mechanical buckling of curved beam under uniformly distributed radial load (in-plane buckling) $F_cr(N)$

Angle	FGM	Isotropic metal	Yang and Kuo [4]	Kang and Yoo [8]	Rajasekaran and Padmanabhan
30	3595	491.31	488.22	478.76	488.13
60	3587	486.54	477.91	464.64	477.66
90	3587	486.54	460.78	432	458.94
180	2940.2	401.63	368.68	276.5	340.32
270	839	113.81	215	94	124.8
360	0	0	0	0	0

Table 2
Mechanical buckling of circular curved beam under pure bending (out-of-plane buckling) $M_cr(N)$

Angle	FGM	Isotropic metal	Vlasov [2]	Papangelis and Trahair [5]	Yang and Kuo [4]
0	−168838	−23125	−23132.6	−23132.6	−23132.6
	168838	23125	23125	23125	23125
30	−41212.8	−5654.83	−5657.2	−5500	−5657.22
	672372.5	91950.8	91950.8	91950.8	91950.8
60	−19764.9	−2715.18	−2713.36	−2411.8	−2713.36
	1282068.2	175305.1	175307	175307	175307
90	−11225.24	−1541	−1541	−1155.77	−1541
	1904681	260428	260432.46	260432.46	260432.46
180	0	0	0	0	0
	3786911.6	517775.67	517774	517774	517783.5
270	6281.9	862.2	862.2	−1077.73	862.22
	5674085	775801.4	775802.3	775802.3	775802.3
360	11308.7	1552.5	1552.5	−4657.7	1552.6
	7562514.4	1033998.6	1034002.4	103366	1034021.5

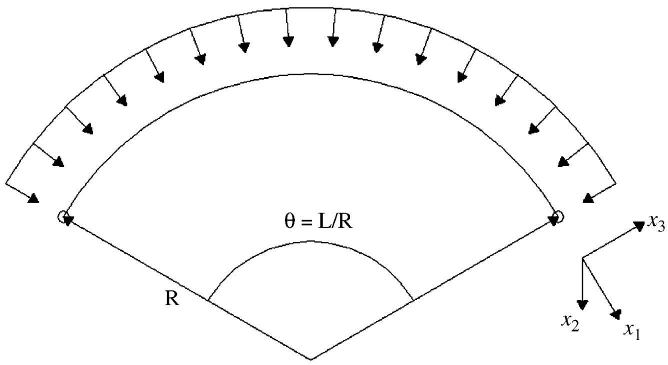

Fig. 2. Curved beam under distributed radial load.

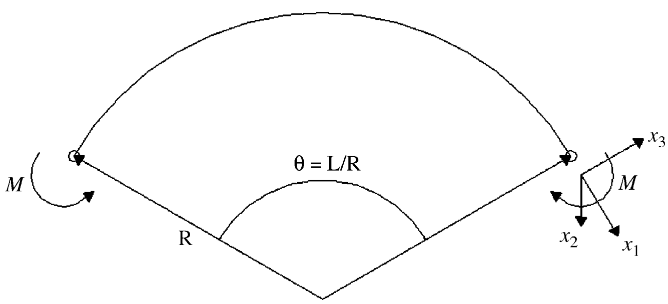

Fig. 3. Curved beam under pure bending (out-of-plane buckling).

for in-plane buckling is compared with those given by Refs. [2,4–6,8] for a doubly symmetric cross section curved beam under in-plane distributed radial load. The numerical results are shown in Table 1. The comparison is well justified.

The out-of-plane buckling bending moment of a FGM curved beam, using the above numerical data, are given in Table 2. Also, to validate the results, the analytical solution presented in this study is reduced for the isotropic material (metal) and the resulting expression for out-of-plane buckling is compared with those given by Refs. [2,4–6,8] for a doubly symmetric cross section curved beam. The comparison is shown in Table 2. The comparison is well justified (Figs. 2 and 3).

7. Conclusion

For spatial stability analysis of circular curved beams, the elastic strain energy and potential energy due to initial stress were derived by applying the principle of virtual work. The Reddy's model for the Young's modules is considered. The analytical solutions were presented for in-plane and out-of-plane buckling of a doubly symmetric cross section FGM curved beam subjected to uniform radial load and pure bending moment under simply supported edge conditions. The following conclusions may be derived:

1. The buckling load for FGM curved beam is greater than the corresponding value for the isotropic metallic curved beam.
2. The results of this study, reduced to the in-plane buckling of a doubly symmetric isotropic simply supported curved beam subjected to uniform compression, is well compared with those reported by Yang and Kuo [4], Rajasekaran and Padmanabhan [6] and Kang and Yoo [8].
3. The analytical results of this paper for the out-of-plane buckling of a doubly symmetric curved beam with simply supported edge conditions subjected to pure bending, when reduced to the metallic curved beam, is well compared with those reported by Yang and Kuo [4], Rajasekaran and Padmanabhan [6] and Kang and Yoo [8].

References

[1] Timoshenko SP, Gere JM. Theory of elastic stability. 2nd ed. New York: McGraw-Hill; 1961.
[2] Vlasov VZ. Thin walled elastic beams. 2nd ed. Washington, DC: National Science Foundation; 1961.
[3] Yoo CH. Flexural-tensional stability of curved beams. Journal of Engineering Mechanics Division, ASCE 1982;108:1351–69.
[4] Yang YB, Kuo SR. Effect of curvature on stability of curved beams. Journal of Structural Engineering, ASCE 1987;113(6):1185–202.
[5] Papangelis TP, Trahair NS. Flexural-torsional buckling of arches. Journal of Structural Engineering, ASCE 1987;113(4):889–906.
[6] Rajasekaran S, Padmanabhan S. Equations of curved beams. Journal of Engineering Mechanics, ASCE 1989;115(5):1094–111.
[7] Yang YB, Kuo SR, Yau JD. Use of straight beam approach to study buckling of curved beams. Journal of Structural Engineering, ASCE 1991;117(7):1963–78.
[8] Kang YJ, Yoo CH. Thin-walled curved beams I: formulation of nonlinear equations. Journal of Engineering Mechanics, ASCE 1994;120(10):2072–101.
[9] Kim M-YBM, Suh MW. Spatial stability of nonsymmetric thin-walled curved beams. Journal of Engineering Mechanics 2000;126(5–8):497–505.
[10] Pi Y-L, Trahair NS. Inelastic lateral buckling strength and design of steel arches. Journal of Engineering Structure 2000;22:993–1005.
[11] Pi Y-L, Trahair NS. In-plane buckling and design of steel arches. Journal of Structure Engineering 1999;125(11):1291–8.
[12] Bradford MA, Pi Y-L. In-plane elastic stability of arches under a central concentrated load. Journal of Engineering Mechanics 2002;128(7):710–9.
[13] Bradford MA, Pi Y-L. Elastic flexural-torsional buckling of discretely restrained arches. Journal of Structural Engineering 2002;128(6):719–27.
[14] Eslami MR, Shahsiah R. Thermal instability of rings made of functionally graded material. In: Proceedings of ASME-ESDA conference, Istanbul, Turkey, July 2002.
[15] Briman V, Suresh S, Mortensen A. Fundamental of functionally graded materials. London: Cambridge Publication; 1998.
[16] Ng TY, Lam YK, Liew KM, Reddy JN. Dynamic stability analysis of functionally graded cylindrical shell under pridic axial loading. International Journal of Solids and Structures 2001;38:1295–300.
[17] Javaheri R, Eslami MR. Thermal buckling of functionally graded plates. AIAA Journal 2002;40(1):162–9.
[18] Javaheri R, Eslami MR. Buckling of functionally graded plates under in-plane compressive loading. ZAMM 2002;82(4):277–83.
[19] Javaheri R, Eslami MR. Thermal buckling of functionally graded plates based on higher-order theory. Journal of Thermal Stresses 2002;25(7):603–25.
[20] Najafizadeh MM, Eslami MR. Thermoelastic stability of circular plates composed of functionally graded materials based on first order theory. AIAA Journal 2002;40(7):1444–50.

[21] Najafizadeh MM, Eslami MR. Thermoelastic stability of orthotropic circular plates. Journal of Thermal Stresses 2002;25(10):985–1005.
[22] Najafizadeh MM, Eslami MR. Buckling analysis of circular plates of functionally graded materials under uniform radial compression. International Journal of Mechanical Sciences 2002;44:2479–93.
[23] Malvern LE. Introduction to the mechanics of a continuous medium. Englewood Cliffs, NJ, USA: Prentice-Hall; 1969.
[24] Praveen GN, Reddy JN. Nonlinear transient thermoelastic analysis of functionally graded ceramic metal plates. International Journal of Solids and Structures 1998;35(33):4457–76.
[25] Eslami MR, Shahsiah R. Thermal buckling of imperfect cylindrical shells. Journal of Thermal Stresses 2001;24(12):1177–98.

Further reading

[1] Reddy JN, Chin CD. Thermomechanical analysis of functionally graded cylinders and plates. Journal of Thermal Stresses 1998;21:593–624;
Fuchiyama T, Noda N, Tsuji T, Obata Y. Analysis of thermal stress and stress intensity factor of functionally gradient materials. Journal of Thermal Stresses 1993;34:75–82.
[2] Nan CW, Yuan RZ, Zhang LM. The physic of metal/ceramic functionally gradient materials. Ceramic Transactions on Functionally Gradient Materials 1993;34:75–82.
[3] Chang SP, Kim MY, Kim SB. Stability of shear deformable thin-walled space frames and circular arches. Journal of Engineering Mechanics, ASCE 1996;122(9):844–54.
[4] Chen H, Blandford GE. Thin walled space frames I: large deformation analysis theory. Journal of Structural Engineering, ASCE 1991;117(8):2499–520.
[5] Kang YJ, Yoo CH. Thin walled curved beams, II: analytical solution for buckling of arches. Journal of Engineering Mechanics, ASCE 1994;120(10):2102–25.
[6] Kuo SR, Yang YB. New theory of buckling of curved beams. Journal of Engineering Mechanics, ASCE 1991;117(8):1698–717.
[7] Kim MY, Chang SP, Kim SB. Spatial stability analysis of thin walled space frames. International Journal of Numerical Methods in Engineering 1996;39(3):499–525.
[8] Yang YB, Kuo SR. Static stability of thin walled curved beams. Journal of Engineering Mechanics, ASCE 1986;112(8):821–41.
[9] Kim MY, Min BC, Suh MW. Spatial stability of nonsymmetric thin walled curved beams. II: numerical approach. Journal of Engineering Mechanics, ASCE 2000;126(5):506–13.
[10] Koizumi M. The concept of FGM. Otsu, Japan: Ryukoku University.
[11] Langhhar HL. Energy methods in applied mechanics. New York: Wiley; 1962.